

Induced Pressure Pumping in Polymer Microchannels via Field-Effect Flow Control

Nathan J. Sniadecki,[†] Cheng S. Lee,[‡] Ponniah Sivanesan,[§] and Don L. DeVoe^{*,†}

Department of Mechanical Engineering, and Bioengineering Program, and Department of Chemistry and Biochemistry, University of Maryland, College Park, Maryland 20742, and Calibrant Biosystems, Rockville, Maryland 20855

Microfluidic field-effect flow control (FEFC) modifies the ζ potential of electroosmotic flow using a transverse electric field applied through the microchannel wall. Previously demonstrated in silicon-based and glass microsystems, FEFC is presented here as an elegant method for flow control in polymer-based microfluidics with a simple and low-cost fabrication process. In addition to direct FEFC flow modulation, independent transverse electric fields in connected microchannels are demonstrated to produce a differential pumping rate between the microchannels. The different electroosmotic pumping rates formed by local ζ potential control induce an internal pressure at the microchannel intersection, resulting in hydrodynamic pumping through an interconnecting field-free microchannel. Modulation of the voltages applied to the gate electrodes adjusts the magnitude and direction of the bidirectional pressure pumping, with fine resolution volume flow rates from -2 to 2 nL/min in the field-free microchannel demonstrated.

Electroosmotic flow (EOF) is a suitable method for bulk fluid pumping in disposable microfluidic systems since it requires no mechanical parts, greatly simplifying device fabrication.^{1–4} An electric field applied longitudinally through a microchannel containing an electrolyte solution generates EOF pumping.⁵ Within a few nanometers from the microchannel wall, a potential difference, known as the ζ potential, develops due to the charge separation of the electrolyte counterions and the surface charge of the wall. For a negative ζ potential, the applied longitudinal electric field drives the accumulated positive counterions at the solution–wall interface electrokinetically toward the cathode. The momentum of the counterions imparts a velocity on the solvent molecules from viscous interactions to produce bulk fluid pumping in the direction of counterion transport.

From the Navier–Stokes relation for incompressible fluid flow with wall-slip boundary conditions, the electroosmotic velocity can be expressed as

$$U_{eo} = -(\epsilon\zeta/\eta)E$$

where ϵ is the dielectric constant, η is the fluid viscosity, E is the longitudinal electric field, and ζ is the zeta potential.⁶ Assuming that the values of ϵ and η remain constant everywhere in the microchannel, then EOF flow direction and magnitude are proportional to both the ζ potential and the applied EOF electric field.

For coupled microchannels in a microfluidic network, adjusting the individual flow velocities in each of the microchannels can be difficult to achieve by changing the applied EOF voltages, due to splitting or summing of the electric fields at the intersections within the network. As one solution to this challenge, surface coatings on glass^{7,8} and plastic^{9–11} substrates have been used to locally modify the ζ potentials, and thus the flow rates, in microchannel systems. However, this method does not allow dynamic control over flow. An alternate method used to dynamically adjust the ζ potential involves applying a transverse electric field through the microchannel wall. The term “field-effect flow control” (FEFC) is used here to describe this technique. The transverse electric field has been generated through fused-silica capillaries^{12–14} and through the walls of microchannels composed of silicon nitride,¹⁵ glass,¹⁶ and thermally grown silicon dioxide.^{17,18} The degree of EOF control is inversely proportional to the wall thickness and proportional to the dielectric constant of the wall material and the applied transverse electric field.¹⁹ Thus, it is critical in FEFC applications for the wall material to exhibit adequate voltage breakdown strength to withstand high transverse electric fields across thin-film walls possessing a relatively high dielectric constant.

FEFC offers several important benefits for bioanalytical applications using polymer microfluidics. In addition to enabling EOF

* To whom correspondence should be addressed: (phone) (301) 405-8125; (fax) (301) 405-3966; (e-mail) ddev@eng.umd.edu.

[†] Department of Mechanical Engineering, and Bioengineering Program, University of Maryland.

[‡] Department of Chemistry and Biochemistry, University of Maryland.

[§] Calibrant Biosystems.

(1) Harrison, D. J.; Manz, A.; Glavina, P. G. *Proc. Int. Conf. Solid-State Sens. Actuators (Transducers '91)*, New York, 1991; pp 792–795.

(2) Harrison, D. J.; Manz, A.; Fan, Z.; Ludi, H.; Widmer, H. M. *Anal. Chem.* **1992**, *64*, 1926–1932.

(3) Jacobson, S. C.; Hergenroder, R.; Koutny, L. B.; Ramsey, J. M. *Anal. Chem.* **1994**, *68*, 1114–1118.

(4) Lazar, I. M.; Karger, B. L. *Anal. Chem.* **2002**, *74*, 6259–6268.

(5) Overbeek, J. T. G. *Electrokinetic Phenomena*; Elsevier: New York, 1952.

(6) Hunter, R. J. *Zeta Potential in Colloid Science: Principles and Applications*; Academic Press: New York, 1981.

(7) Ramsey, R. S.; Ramsey, J. M. *Anal. Chem.* **1997**, *69*, 1174–1178.

(8) Culbertson, C. T.; Ramsey, R. S.; Ramsey, J. M. *Anal. Chem.* **2000**, *72*, 2285–2291.

(9) Barker, S. L. R.; Ross, D.; Tarlov, M. J.; Gaitan, M.; Locascio, L. E. *Anal. Chem.* **2000**, *72*, 5925–5929.

(10) Liu, Y.; Fanguy, J. C.; Bledsoe, J. M.; Henry, C. S. *Anal. Chem.* **2000**, *72*, 5939–5944.

(11) Wang, S.-C.; Perso, C. E.; Morris, M. D. *Anal. Chem.* **2000**, *72*, 1704–1706.

(12) Lee, C. S.; Blanchard, W. C.; Wu, C.-T. *Anal. Chem.* **1990**, *62*, 1550–1552.

(13) Hayes, M. A.; Ewing, A. G. *Anal. Chem.* **1992**, *64*, 512–516.

(14) Hartley, N. K.; Hayes, M. A. *Anal. Chem.* **2002**, *74*, 1249–1255.

control using only low-voltage signals for general micropumping needs in disposable plastic chips, the use of differential electroosmosis is promising for localized pressure pumping in microfluidic networks. Capillaries with two different ζ potential regions, hence differential EOF pumping rates, generate a hydrostatic pressure at the intersection of the two regions in order to satisfy continuity.²⁰ Visualization experiments of caged fluorescent dye in coupled capillaries show that parabolic flow profiles exist in the capillaries due to the pressure induced at the capillary union.²¹ Similar velocity profiles results were confirmed with finite element modeling of a T-channel intersection with differential ζ potentials.²²

Beyond general on-chip micropumping applications, FEFC technology also provides the ability to fine-tune EOF velocities during biomolecular separations. For example, it is important to control the magnitude and direction of EOF when performing electrophoretic or chromatographic separations in order to control the precision of analyte migration times and to maximize separation efficiency and resolution. Furthermore, when performing multiple separations across different chips, or parallel separations on a single chip, maintaining the same EOF conditions for all separations is critical to ensure uniform results from each separation channel. Significant nonuniformities in EOF within microfluidic systems can occur naturally as a result of variations in as-fabricated channel dimensions and surface properties, variations in postfabrication surface modifications and analyte adsorption, and variations in buffer conditions. FEFC thus provides a mechanism for dynamic control of EOF, with the potential to optimize separation efficiency and resolution while improving uniformity across multiple separations, all through the application of only low-voltage bias signals.

This paper reports the use of FEFC to dynamically modulate the ζ potential in a polymer microchannel network. Pressure-driven flow in a field-free microchannel located at the T-intersection of two microchannels with separate FEFC gate electrodes results from the differential EOF pumping rates. Figure 1 depicts the cross-sectional layout along the two main microchannels and shows representational velocity profiles from the modulated ζ potentials due to FEFC in the main microchannels. As illustrated in Figure 2, varying the FEFC gate voltages under constant longitudinal EOF electric field strength manipulates the magnitude and direction of the pressure-driven flow velocity in the field-free microchannel.

In addition to the use of differential EOF for generating pressure-driven flow, this work demonstrates FEFC in a plastic microfluidic system. The use of plastic materials for microfluidic applications shows great promise for the realization of disposable bioanalytical platforms. Plastics that are popular for use in microfluidics include poly(carbonate) (PC),^{23–25} poly(dimethylsi-

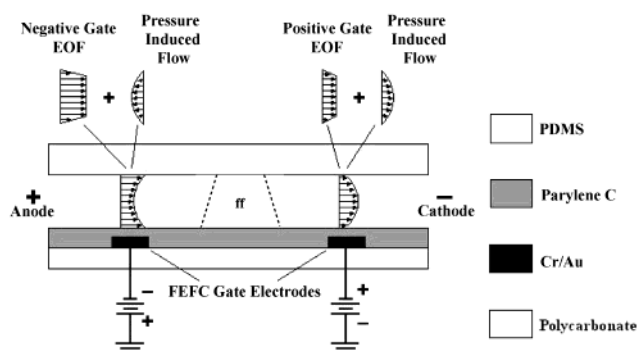


Figure 1. Cross-sectional schematic of the FEFC gate electrodes in a T-intersection microchannel network. The field-free microchannel (ff) is shown between the two FEFC gate electrodes.

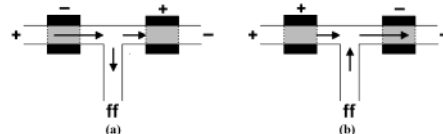


Figure 2. Differential EOF pumping rates from gate voltages applied to the FEFC electrodes producing (a) positive pressure for flow down and (b) negative pressure for flow up the field-free microchannel (ff).

loxane) (PDMS),^{26–28} poly(ethylene terephthalate),^{23,29} poly(methyl methacrylate),^{30,31} polystyrene,³² and SU-8.³³ A promising plastic for disposable bioanalytical platforms is Parylene C, which is a vapor-deposited polymer with fine film-thickness control that can be used as a conformal coating with no residual film stresses. It has been used in numerous microfluidic applications for microchannel structures,³⁴ electro-spray tips,³⁵ microcheck valves,³⁶ and integrated on-chip detectors.³⁷ Compared to other polymers, Parylene C offers particular advantages for polymer-based FEFC devices due to its highly conformal thin-film deposition, moderate dielectric constant, and relatively high voltage breakdown strength.³⁸

- (15) Schasfoort, R. B. M.; Schlautmann, S.; Hendrikse, J.; van den Berg, A. *Science* **1999**, *286*, 942–945.
- (16) Polson, N.; Hayes, M. A. *Anal. Chem.* **2000**, *72*, 1088–1092.
- (17) Buch, J. S.; Wang, P.-C.; DeVoe, D. L.; Lee, C. S. *Electrophoresis* **2001**, *22*, 3902–3907.
- (18) Sniadecki, N. J.; Wang, P.-C.; Lee, C. S.; DeVoe, D. L. *Proceedings Micro Total Analysis Systems 2001*, Monterey, CA, 2001; pp 187–188.
- (19) Lee, C. S.; McManigill, D.; Wu, C.-T.; Patel, B. *Anal. Chem.* **1991**, *63*, 1519–1523.
- (20) Chien, R.-L.; Helmer, J. C. *Anal. Chem.* **1991**, *63*, 1354–1361.
- (21) Herr, A. E.; Molho, J. I.; Santiago, J. G.; Mungal, M. G.; Kenny, T. W.; Garguilo, M. G. *Anal. Chem.* **2000**, *72*, 1053–1057.
- (22) Bianchi, F.; Ferrigno, R.; Girault, H. H. *Anal. Chem.* **2000**, *72*, 1987–1993.

- (23) Roberts, M. A.; Rossier, J. S.; Bercier, P.; Girault, H. *Anal. Chem.* **1997**, *69*, 2035–2042.
- (24) Yingjie, L.; Ganser, D.; Schneider, A.; Liu, R.; Blackwell, J.; Fayden, D.; Weston, D.; Rhine, D.; Smekal, T.; Grodzinski, P. *Proc. Int. Conf. Solid-State Sens. Actuators (Transducers '01)*, Munich, Germany, 2001; pp 1170–1173.
- (25) Klintberg, L.; Svedberg, M.; Nikolajeff, F.; Thornell, G. *Sens. Actuators, A* **2003**, *103*, 307–316.
- (26) Duffy, D. C.; McDonald, J. C.; Schueller, O. J. A.; Whitesides, G. M. *Anal. Chem.* **1998**, *70*, 4974–4984.
- (27) Effenhauser, C. S.; Bruin, C. J. M.; Paulus, A.; Ehrat, M. *Anal. Chem.* **1997**, *69*, 3451–3457.
- (28) Terray, A.; Oakley, J.; Marr, D. W. M. *Science* **2002**, *296*, 1841–1844.
- (29) Rossier, J. S.; Roberts, M. A.; Ferrigno, R.; Girault, H. H. *Anal. Chem.* **1999**, *71*, 4294–4299.
- (30) Martynova, L.; Locascio, L. E.; Gaitan, M.; Kramer, G. W.; Christensen, R. G.; MacCrehan, W. A. *Anal. Chem.* **1997**, *69*, 4783–4789.
- (31) Yuen, P. K.; Kricka, L. J.; Wilding, P. J. *Micromech. Microeng.* **2000**, *10*, 401–409.
- (32) Truckenmuller, R.; Rummler, Z.; Schaller, T.; Schomburg, W. K. *J. Micro-mech. Microeng.* **2002**, *12*, 375–379.
- (33) Guerin, L. J.; Bossel, M.; Demierre, M.; Calmes, S.; Renaud, P. *Proc. Int. Conf. Solid-State Sens. Actuators (Transducers '97)*, Chicago, IL, 1997; pp 1419–1422.
- (34) Selvaganapathy, P.; Ki, Y.-s. L.; Renaud, P.; Mastrangelo, C. H. *J. Micro-electromech. Syst.* **2002**, *11*, 448–453.
- (35) Licklider, L.; Wang, X.-Q.; Desai, A.; Yu-Chong, T.; Lee, T. D. *Anal. Chem.* **2000**, *72*, 367–375.
- (36) Wang, X.-Q.; Tai, Y.-C. *Proc. IEEE Int. Conf. Micro Electro Mech. Syst.*, Miyazaki, Japan, 2000; pp 68–73.

EXPERIMENTAL SECTION

Fabrication. The FEFC gate electrodes were deposited on PC substrates (Sheffield Plastics Inc., Sheffield, MA) with 200 Å of Cr and 3500 Å of Au evaporated onto the surface. The metal was patterned with standard lithography techniques, and the exposed metal areas were removed with aqueous Au and Cr etchants (Transene, Danvers, MA). While solvents present in commercial photoresist are known to damage PC substrates,³⁹ the metallization used here is sufficiently thick to prevent solvent diffusion to the PC surface. Parylene C was deposited to a thickness of 1.22 μm on the entire wafer surface using a dedicated vapor-phase system (Specialty Coating System, Indianapolis, IN).

The microchannels were molded from PDMS (Sylgard 184, Dow Corning, Midland, MI) that was poured onto a silicon wafer master and cured to replicate the microstructures on the silicon master. The master mold was fabricated by bulk etching of a 100-mm silicon wafer coated with a 2-μm thermal silicon dioxide layer (Silicon Quest Intl., Santa Clara, CA). Two microchannel layout designs were fabricated—a straight microchannel for direct polymer FEFC characterization and a T-intersection microchannel network for induced pressure pumping. After patterning with photolithography, the silicon dioxide was etched with 5:1 buffered oxide etchant (J.T. Baker, Phillipsburg, NJ) and the underlying bulk silicon was etched in anisotropic silicon etchant (Transene, Danvers, MA) at 60 °C. After pouring the PDMS on the master mold, it was cured for 2 h at 60 °C in a convection oven. The PDMS microchannels used in this work were trapezoidal in cross-sectional shape with a height of 45 μm and widths varying from 100 (top) to 165 μm (bottom) due to the angled sidewall geometry of the silicon master mold.

Current Monitoring. To characterize the modulated EOF velocity due to FEFC, current monitoring was performed in the straight microchannel. The approach follows the work of Zare et al.,⁴⁰ with the time history of current measured as electrolytes of different concentrations, and thus different conductivities, migrate through the microchannel due to EOF. Three power supplies (E-3612A, Agilent, Palo Alto, CA) were used to apply the electric field between the reservoirs and voltage bias to the single FEFC gate electrode. The current-monitoring experiments were performed on a probe station (REL-4800, Cascade Microtech, Beaverton, OR). The micromanipulators were fitted with Pt electrodes (Fisher Scientific, Pittsburgh, PA) to make contact with the buffer solution in the reservoirs, and a tungsten probe tip was used to make electrical contact to the FEFC gate electrode. The current was recorded by reading the voltage drop across a 1-MΩ resistor with a data acquisition unit (34970A, Agilent). The modulated EOF velocity was measured from the time it took the current to reach a steady-state value as the low concentration buffer solution replaced a high-concentration solution in the microchannel.

Flow Visualization. Fluorescent microbeads were individually recorded in the microchannel network for velocity measurements of the induced pressure pumping at the T-intersection. The image recording was performed on a Nikon TE-2100-S fluorescent

inverted microscope (Nikon) using a B-2E/C FITC filter (excitation 465–495 nm, emission 515–555 nm). Two power supplies were used to apply the EOF electric field, and three power supplies were used for the two FEFC gate electrodes. For the experiments, the three-gate power supplies were set to a positive gate voltage, a negative gate voltage, and zero gate voltage, respectively. Control of which power supplies biased the two-gate electrodes was performed with LabView software (National Instruments, Austin, TX), a multiplexer card (PCI-6711, National Instruments), and two relays (MR62-6S, NEC Tokin, Seoul, Korea). The bias voltages of the FEFC gate electrodes were switched at 10-s intervals between four voltage configurations. A 640 × 480 pixel CCD camera (DKF-4303, The Imaging Source, Charlotte, NC) was used to record the flow of the microbeads in the microchannels at 30 frames/s.

Postprocessing of the velocity measurements was performed with the aid of the Image Processing Toolbox in Matlab (The Mathworks, Natick, MA). A Sobel edge detection method was used to determine boundary pixels of each of the microbeads. The position of the center pixel for each of the microbeads was measured every 10 image frames, corresponding to a 0.33-s time interval. A scale conversion of 0.75 μm/pixel was used to measure the position of the microbeads in each frame. The velocity for each voltage configuration of the FEFC gate electrodes was determined from the slope of a linear best-fit line through the position measurements.

Reagents. Acetic acid buffer solutions (Fisher Scientific, Pittsburgh, PA) for the current monitoring experiments were prepared to 10 and 20 mM concentrations and adjusted to pH 3.1 using hydrochloric acid. For the flow visualization experiments, 2.0-μm-diameter polystyrene microparticles (Fluorobrite beads, Polysciences, Warrington, PA) were treated for 12 h in 25 mM Fe(NH₄)₂(SO₄)₂·6H₂O (Fisher Scientific) to reduce their surface charge, eliminating their electrophoretic mobility that would otherwise interfere with the EOF measurements. The microbeads were filtered from the Fe solution with a syringe filter (0.45-μm MCE filter, Fisher Scientific), rinsed with deionized water, and extracted into 2 mM acetic acid buffer at pH 3.8 to be used for the flow visualization experiments.

RESULTS AND DISCUSSION

FEFC Characterization. The EOF is directly proportional to the applied transverse electric field from the voltage applied at the gate underneath the Parylene C microchannel wall. The double capacitor theory¹⁹ states that the change to the zeta potential, Δζ, due to FEFC can be approximated by

$$\Delta\zeta = (C_W/C_D)(V_G - V_C) \quad (1)$$

where C_W is the wall capacitance, C_D is the diffuse layer capacitance, V_G is the voltage applied to the FEFC gate, and V_C is the voltage in the microchannel at the FEFC gate due to the applied longitudinal electric field. In the experiments, V_C varies linearly along the microchannel, with $V_C = 0$ at the midpoint between the anodic and cathodic reservoirs, so that the average change in the ζ potential may be expressed as $\Delta\zeta = C_W/C_D V_G$. For an applied negative gate voltage, the change in the ζ potential is negative, resulting in larger EOF velocity in the microchannel.

(37) Webster, J. R.; Burns, M. A.; Burke, D. T.; Mastrangelo, C. H. *Anal. Chem.* **2001**, *73*, 1622–1626.

(38) *Encyclopedia of Chemical Technology*, 4th ed.; *Supplement Volume: Aerogels to Xylylene Polymers*; Howe-Grant, M., Ed.; Wiley: New York, 1998.

(39) Kimball, C.; DeVoe, D. L. *Micro Total Analysis Systems 2002*, Nara, Japan, 2002; pp 724–726.

(40) Huang, X.; Gordon, M. J.; Zare, R. N. *Anal. Chem.* **1988**, *60*, 1837–1938.

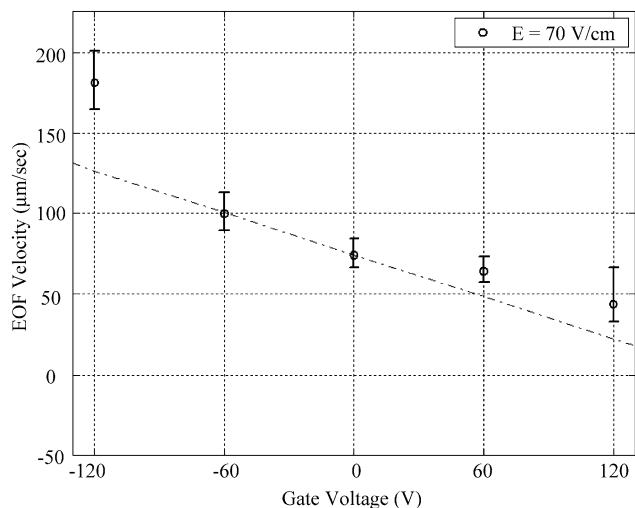


Figure 3. EOF mobility measurements versus voltage applied to a single FEFC gate electrode in a straight microchannel from current monitoring of 10 mM/20 mM acetic acid buffer solution at pH 3.1. The theoretical double capacitor linear relationship is plotted (dashed-dot, - - -) for comparison.

Likewise, for a positive gate voltage, the EOF velocity will be reduced. To investigate the feasibility of Parylene C as an effective material for FEFC, the EOF velocity was measured by current monitoring for positive and negative gate voltages in a straight PDMS microchannel. The bottom microchannel wall was composed of Parylene C, and a single FEFC gate spanned the full length of the microchannel.

Initial tests to evaluate baseline FEFC performance used a 1.70-cm-long microchannel with a FEFC gate electrode of equal length. Current monitoring was used to determine average flow velocity. All experiments were carried out in acetic acid buffer at pH 3.1. Acetic acid is an excellent buffer solution for low-pH applications and is commonly used for capillary zone electrophoresis and capillary isotachopheresis separations of peptides. The Pt electrode in the anodic reservoir was biased at +60 V. The Pt electrode at the cathodic reservoir was connected in series with the resistor and with a power supply biased at -60 V. The change in voltage across the resistor was monitored with the data acquisition unit to determine the flow velocity in the microchannel. This configuration resulted in an applied longitudinal EOF electric field of 70.5 V/cm. The third power supply was used to bias the FEFC gate, applying the transverse electric field to generate FEFC. The EOF was allowed to reach a steady state for 10 min prior to beginning each test. Five FEFC gate voltages were analyzed ranging from -120 V to +120 V. Since current monitoring is known to result in substantial uncertainty in velocity measurements, all EOF experiments were repeated five times at each gate voltage to improve confidence in the average measurements. The measured velocities with error bars are given in Figure 3.

Applying the double capacitor theory for the microchannel wall thickness $t = 1.22 \mu\text{m}$ and relative permittivity $\epsilon_r = 3.15$ for Parylene C, the wall capacitance is

$$C_W = (\epsilon_r \epsilon_0 / t) = 2.29 \times 10^{-5} \text{ (F/m}^2\text{)}$$

For an average buffer concentration of $c = 15 \text{ mM}$ with valence

$z = 1$ for acetic acid buffer solution and an unmodified ζ potential of $\zeta_0 = -13.5 \text{ mV}$, the diffuse layer capacitance⁶ is

$$C_D = 2.285z\sqrt{c} \cosh(19.46z\zeta_0) = 0.236 \text{ (F/m}^2\text{)}$$

Thus, the theoretical velocity control slope for the applied gate voltages is equivalent to $-0.435 \mu\text{m (V}\cdot\text{s)}^{-1}$, and this relationship is plotted along with the experimental results in Figure 3. The experimental results agree with the linear relationship with some deviation at high negative gate voltages.

It should be noted that the microchannels used in this experiment were fabricated using two microchannel wall materials, namely, Parylene C above the FEFC gate and PDMS surrounding the remaining three channel walls. Thus, while the applied gate voltage directly affects the ζ potential of the Parylene C layer, it is not known how the ζ potential of the PDMS walls will change. The disagreement between experimental and theoretical velocities at higher gate voltages may be a result of this constraint.

Differential EOF Characterization. Voltages applied to the FEFC gates modulated the local ζ potentials in two connected microchannels inducing pressure pumping due to the differential electroosmosis. The induced pressure pumping was studied with a microfluidic network consisting of three microchannels at a T-intersection as shown in Figure 1 and Figure 2. The microchannel length between anodic and cathodic reservoirs was 1.83 cm, and the length of the field-free microchannel was 0.54 cm. Two independent FEFC gate electrodes, each with a length of 2 mm and positioned at a distance of 1.5 mm from the intersection, were used to modify the ζ potential in the anodic and cathodic microchannels. The field-free microchannel did not have a FEFC gate electrode, and its reservoir was kept at a floating potential to ensure no EOF in the microchannel. The EOF electric field was held constant at 30.1 V/cm between the anodic and cathodic reservoirs for all tests. The microchannels were filled with acetic acid buffer solution at pH 3.8, and neutralized fluorescent microbeads were injected into the anodic reservoir to begin the flow visualization analysis. As illustrated in Figure 4, a voltage sequence of the FEFC gate voltages was initiated in LabView to automate the modulation of the ζ potentials during the experiments. Because the $2\text{-}\mu\text{m}$ polystyrene beads were neutralized to eliminate electrophoretic mobility, deposition of beads onto the channel walls was a concern. To prevent deposited beads from significantly affecting the baseline ζ potentials of the Parylene C or PDMS surfaces, extremely low bead concentrations were used in these experiments.

The generation of negative or positive induced pressure was instantaneous to the change in applied FEFC gate voltage. The microbeads in the field-free microchannel flowed away from the intersection when the gate voltage in the anodic microchannel was lower than that of the gate voltage in the cathodic, due to a positive hydrostatic induced pressure at the intersection. Likewise, the microbeads in the field-free microchannel flowed toward the intersection when the cathodic gate voltage was greater than that of the anodic due to a negative induced pressure. The plot of average velocity and microbead position measurements over time in Figure 5 illustrates the bidirectional switching of the field-free flow rate for a test conducted at +70 and -70 V applied to the FEFC gates. The results for the tests show that the flow in the

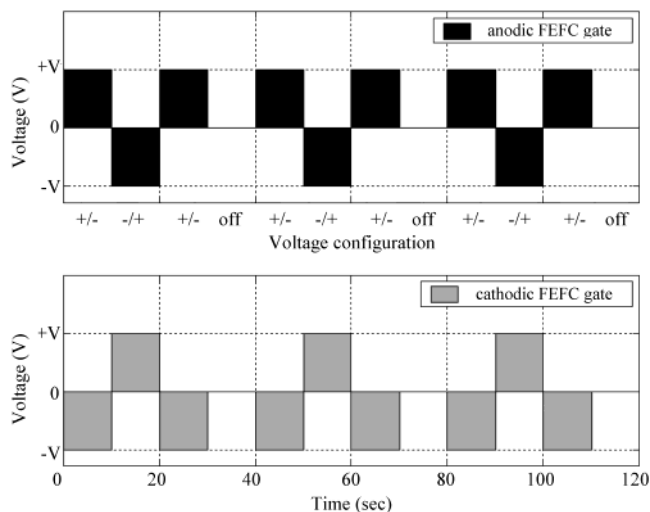


Figure 4. Voltage control sequence loop applied to the FEFC gates to produce flow up (+/-), flow down (-/+), and no flow (off) in the field-free microchannel. The time between FEFC voltage configurations is 10 s. Voltages of ± 90 , ± 70 , and ± 50 V were used in the tests.

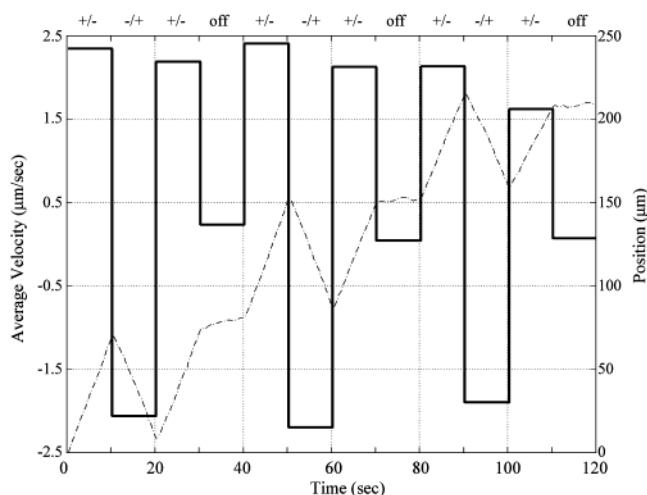


Figure 5. Microbead velocity measured from video particle tracking in the field-free microchannel from differential EOF of 2 mM acetic acid buffer solution at pH 3.8 for ± 70 V gate voltages. The average velocity (solid, —) and the microbead position (dashed-dot, - · -) are plotted versus time (bottom axis) and FEFC gate configuration (top axis).

field-free microchannel could be switched with reasonable repeatability. With zero gate voltages applied to the FEFC gate electrodes, the microbeads exhibited negligible flow in the field-free microchannel due to the lack of induced pressure as expected for equal EOF pumping rates.

The induced pressure also affected the microbead flow in the anodic and cathodic microchannels. During tests at +90 and -90 V gate voltages, the FEFC gate voltages were switched to generate negative pressure when a tracked microbead was in the anodic microchannel, causing its velocity to increase from 72.5 to 80.2 $\mu\text{m/s}$ due to the induced pressure pumping toward the T-intersection. After the microbead crossed over the intersection and into the cathodic microchannel, the gate voltages were switched to +90 V at the anodic FEFC gate and -90 V at the cathodic and the microbead velocity increased from 64.4 to 70.9

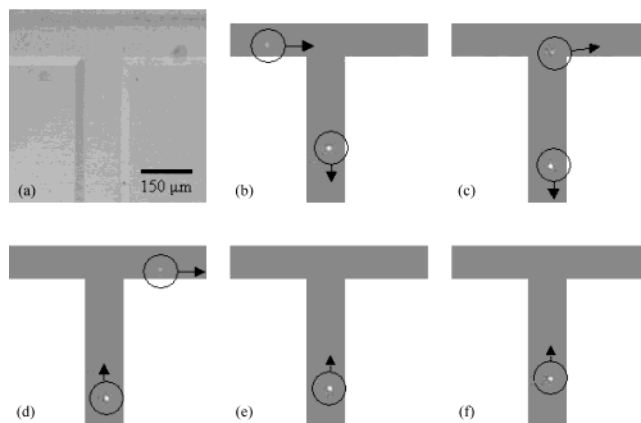


Figure 6. FEFC gate voltages of -90 V at the anodic gate and $+90$ V at the cathodic gate produced flow down the field-free microchannel in the first row of images (a–c). At 13.9 s (image d), the voltages were switched to $+90$ V at the anodic FEFC gate and -90 V at the cathodic FEFC gate inducing flow up the field-free microchannel in the second row of images (d–f). For both gate configurations, the top microbead continues toward the cathodes.

$\mu\text{m/s}$ due to the positive pressure pumping. Figure 6 shows a sequence of images taken at the T-intersection where a microbead in the anodic and cathodic microchannels continues toward the cathode while a microbead in the field-free microchannel changes flow direction when the FEFC gate voltages are switched. For voltage breakdown of the Parylene C or high charge leakage, the additional longitudinal electric fields would be greater than that of the EOF electric field due to the applied gate voltages and distances between FEFC electrodes and/or the reservoirs. In particular, for a negative gate voltage in the anodic microchannel and positive gate voltage in the cathodic microchannel, the microbead flow direction in the main microchannels would be reversed with the onset of electrical breakdown or charge leakage. For all the tested gate voltages, the absence of observed flow reversal in the anodic and cathodic microchannels during the FEFC gate switching shows that the gate electrodes influence only the ζ potential but not the EOF electric field.

As expected, the average velocity in the field-free microchannel was found to be linearly dependent on the difference between the voltages applied to the FEFC gates. Using a voltage control sequence loop, the induced pressure pumping was characterized for three voltage pairs (± 90 , ± 70 , ± 50 V) applied to the FEFC gate electrodes and an “off” configuration (0 V). The average flow rates are plotted in Figure 7 along with a best-fit line. For simplification of the microchannel flow, the trapezoidal sidewalls were modeled as rectangular for theoretical comparison. The flow rate for incompressible, steady flow in a rectangular cross section⁴¹ without electrokinetic forces is

$$Q = \frac{4ba^3}{3\mu} \left(-\frac{\partial p}{\partial x} \right) \left[1 - \frac{192a}{\pi^5 b} \sum_{i=1,3,5,\dots}^{\infty} \frac{\tanh(i\pi b/2a)}{i^5} \right] \quad (2)$$

where $2a$ is the distance between sidewalls, $2b$ is the distance between top and bottom walls, and $\partial p/\partial x$ is the pressure gradient. For a positive induced pressure at the T-intersection, the pressure

(41) White, F. M. *Viscous Fluid Flow*; McGraw-Hill: New York, 1991.

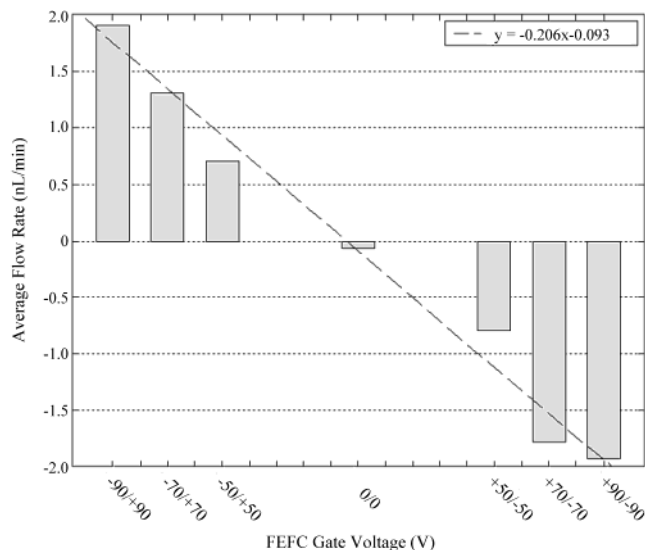


Figure 7. Average induced pressure pumping rates in the field-free microchannel for FEFC gate voltage configurations. Positive flow rate is toward the field-free reservoir, and the best-fit line is shown (dashed, - -) for comparison.

gradient along the field-free microchannel is negative, canceling the negative sign in the coefficient to produce mass flow toward the field-free reservoir. The flow rate equation suggests a linear relationship between the flow in the microchannel and the induced pressure at the T-intersection. Solving for the pressure gradient in eq 2, maximum negative and positive pressure gradients of -36.0 and 36.1 Pa/m were determined from the experimental flow rates.

During the tests, a small inherent pressure difference existed between the field-free reservoir and the intersection that resulted in a measurable microbead velocity of the microbeads in the field-free microchannel for equal voltages applied to the FEFC gate

electrodes. This is shown in the graph as a small negative pumping rate for equal gate voltages (0 V). For all tests, the induced pressure from the FEFC gate voltages was sufficient to counteract this flow and thus change the velocity of the microbeads.

CONCLUSIONS

A polymer-based FEFC micropump has been successfully demonstrated and characterized for dynamic control of pressure induced pumping. The pumping mechanism has been shown to enable fully bidirectional hydrodynamic flow by coupling multiple FEFC gate electrodes in a microchannel network for differential EOF. This flow control technique does not require adjustment of the reservoir pressure or manipulation of the longitudinal EOF electric fields at the fluid reservoirs, nor does it need complex methods to dynamically modify the microchannel surface chemistry. Pumping rates from approximately -2 to 2 nL/min were readily achieved in the field-free microchannel using differential EOF in the anodic and cathodic microchannels. Differential EOF by means of FEFC makes tunable pumping possible at internal nodes within microfluidic networks, providing dynamic flow control within field-free microchannels.

ACKNOWLEDGMENT

This research is supported by National Institutes of Health Grants GM62738 and EB000453, Defense Advanced Research Projects Agency Contract 02SB1-0232, and the Maryland Industrial Partnerships (MIPS) program. The authors appreciate the fabrication assistance of Tom Loughran at the University of Maryland's Electrical Engineering Cleanroom and Mike Beamesderfer at NASA Goddard Space Flight Center, Greenbelt, MD.

Received for review July 11, 2003. Accepted January 28, 2004.

AC034783T